Chapter 2

Synthesis and Characterization of Adduct Modified Clay and Polystyrene Clay Nanocomposites

2.1. ABSTRACT

The first part of the present chapter deals with the synthesis of Adduct modified clay (AMC) having different reactive acid group like acrylic acid, cinammic acid and oleic acid. A facile method is adopted for the modification of Na^+-MMT using Acid-Amine adducts. The successful clay modification via cation exchange was confirmed by FT-IR spectroscopy and X-ray diffraction (XRD). GPC (Gel permeation chromatography) analysis was carried out to find the molecular weight distribution of polystyrene in polystyrene clay nanocomposite. In the second part, these Adduct modified clay (AMC) with reactive functionality was used for the preparation of polystyrene clay nanocomposite (PSC). A series of discrete nanocomposite particles of PSC using 10 wt.% AMC were prepared by effectively dispersing the inorganic MMT clay platelets in organic polystyrene (PS) matrix via *in situ* intercalative polymerisation. The as-synthesized neat PSC materials were characterized by FT-IR spectroscopy, XRD, thermogravimetric analysis (TGA) and differential scanning calorimetry (DSC).

2.2. INTRODUCTION

Clay continues to receive significant attention for its ability to impart mechanical reinforcement (Ojijo et al., 2012; Pavlidou et al., 2008; Bindu et al.,

2014; Hou et al., 2011), gas barrier (Cui et al., 2015; Feldman., 2013; (Gorrasi et al., 2003; Lange and Wyser., 2003; Tan and Thomas., 2016) and even flame retardant characteristics to polymers (Wang et al., 2003; Kashiwagi et al., 2004; Qin., et al., 2005; Kiliaris and Papaspyrides., 2010). As a consequence, a wide range of engineering properties can be significantly improved with a low level of filler loading, typically less than 5 wt%. At such a low loading level, polymers such as nylon-6 show an increase in Young's modulus of 103%, in tensile strength of 49%, and in heat distortion temperature of 146% (Kojima et al., 1993). Also because of the low price, availability, high aspect ratio as well as desirable nanostructure and interfacial interactions, clays can provide dramatic and adjustable improved properties at very lower loadings without the sacrificing of pure polymer processability. To prevent aggregation, the clay concentration rarely exceeds 10 wt % in traditional polymer clay composites (Arroyo et al., 2003, Yasim et al., 2003; Gao, 2004). In order to promote clay dispersion in polymer matrices, organically modified clays or organoclays are commonly used, providing strong interaction between polymers and nanoparticles which facilitates formation of intercalated and/or exfoliated morphologies (Su and Wilkie, 2003). Organic compounds used to prepare organoclays include quaternary ammonium salts (Maiti et al., 2002; Tang et al., 2003; Kozak and Domka., 2004), nonionic surfactants (Gemeay et al., 2002; Yao et al., 2002; Bottino et al., 2003), biomemolecules etc..

For these reasons, polymer clay nanocomposites are superior to conventional composites, and make them competitive with other materials for a wide range of applications. Recently, some polymer clay nanocomposites became

commercially available, and were applied to the automotive (Garces et al., 2000) and food packaging industries. Biodegradable polymer based nanocomposites appear to have a very bright future for a wide range of applications as high performance biodegradable materials (Sinha and Okamoto et al., 2003a; Ray et al., 2002). Although a significant amount of work has already been done on various aspects of polymer clay nanocomposites, much research still remains in order to understand the complex structure–property relationships in various nanocomposites. Nowadays the use of organoclays as precursors to nanocomposite preparation has been extended into large variety of polymer systems including vinyl polymers (Okamoto et al., 2001; Zeng et al., 2002; Beyer et al., 2002; Nisha et al., 2000; Fournaris et al., 1999), condensation (step) polymer (Kojima et al., 2003; Zhang et al., 2008), polyolefins (Hasegawa et al., 1998; Somwangthanaroj et al., 2003 Morgan and Harris, 2003), specialty polymers and biodegradable polymers(Sinha et al., 2002; Sinha et al., 2003).

Recently, Nair et al., 2010 reported the synthesis of polystyrene clay nanocomposite using POSS modified clay. Silanes used for the preparation of POSS solution was very costly and the procedure used for the composite preparation was found to be time consuming and tedious. So for further applications, we require a cost effective and facile method for clay modification and composite preparation.

Hence, in this present chapter, our aim was to synthesize a facile, cost effective method for clay modification using different Acid-Amine adducts having reactive sites. Adducts were prepared by treating equimolar concentration of different unsaturated acid with Quaternary ammonium salt (Cetyl Trimethyl

Ammonium Bromide) and polystyrene clay nanocomposite (PSC) materials were prepared using these adduct modified clay (AMC) via *in situ* intercalative polymerisation. The nanocomposites as synthesized were characterised by FT-IR spectroscopy, XRD, thermogravimetric analysis (TGA) and differential scanning calorimetry (DSC).

2.3. EXPERIMENTAL

2.3.1. Materials

Styrene monomer (99%), Oleic acid (OA), Acrylic acid (AA), Cinnamic acid (CC) and Cetyl Trimethyl Ammonium Bromide (CTAB) was purchased from Sigma-Aldrich Chemicals, USA. The clay used in this work was sodium montmorillonite, (Na^+-MMT) (Cation exchange capacity (CEC) 92.6 meq/100g) purchased from Southern Clay Products. The initiator Benzoyl peroxide (BPO) from S.D. Fine Chemical Ltd., India and was recrystallized from ethanol before using. Ethanol, Methanol, Toluene and Tetrahydrofuran (THF) of HPLC grade were obtained from Merck Specialties Pvt. Ltd., India. Styrene was then washed with 5 % sodium hydroxide solution to remove the inhibitor, followed by repeated washing with distilled water to remove the alkali and finally distilled under reduced pressure. The inhibitor free monomer was stored under ice-cold conditions.

2.3.2. Methods

2.3.2.1. Synthesis of Adduct Modified Clay

Adduct modified clay (AMC) were synthesized via cation exchange of Na^+ with adducts. Adducts were prepared by treating equimolar

concentration of Cetyl Trimethyl Ammonium Bromide (CTAB) with unsaturated organic acids like Acrylic acid (AA), Cinnamic acid (CA) and Oleic acid (OA). The hydroxyl group of an acid react to form adduct with CTAB (quaternary ammonium salt), were as olefinic part of the unsaturated acid is used for the polymerization reaction. 1 g of clay (cation exchange capacity (CEC) = 92.6 meq/100g) was dispersed in 200 mL of distilled water and stirred for 1 h until a homogeneous mixture was formed. Pre-dissolved equimolar concentration of the Acrylic acid-CTAB mixture (equivalent to 2 CEC of the clay) was slowly added to the clay suspension at ambient conditions and stirred uninterrupted for 48 h. The resulting AMC suspension was recovered by ultra-centrifuging at 5000 rpm for 30 min. Product purification was done through washing and ultra-centrifuging the sample repeatedly with ethanol to remove the excess of intercalating agent. Finally, the modified clay was dried overnight in a vacuum oven at 80°C to obtain Acrylic acid-CTAB adduct modified clay and was designated as (AC-AMC). The flow chart for clay modification using Acid-CTAB adduct was given in Figure 2.1.

The same procedure was used to prepare Cinnamic acid-CTAB and Oleic acid-CTAB adducts modified clay. The resultant modified clays were identified as (CC-AMC) and (OC-AMC), respectively. The structures of adducts used in this study were shown in Figure 2.2.

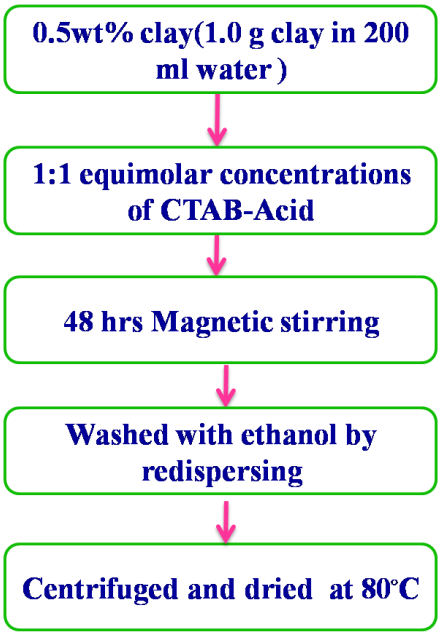

Figure 2.1. Flow chart for clay modification

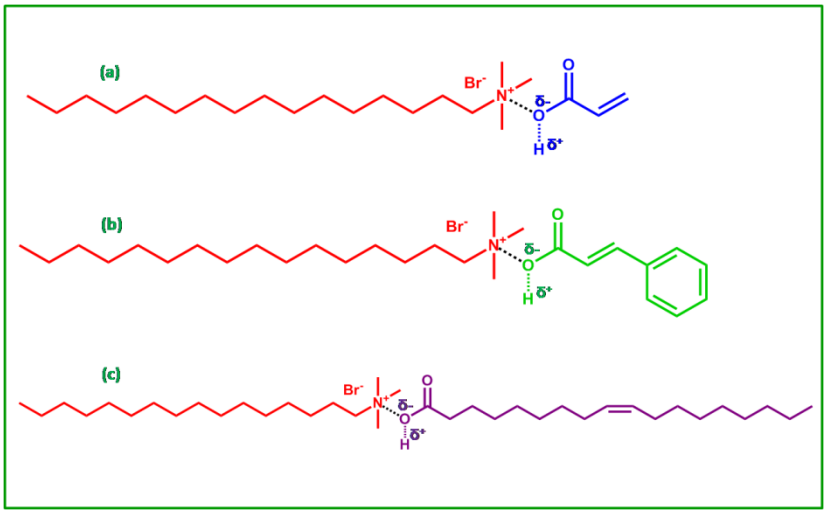

Figure 2.2. Structure of adducts (a)Acrylicacid-CTAB adduct, (b) Cinnamic acid-CTAB adduct and (c) Oleic acid-CTAB adduct

2.3.2.2. Synthesis of Polystyrene Clay Nanocomposite

The Polystyrene clay nanocomposite (PSC) was synthesized by in-situ intercalative polymerization of styrene using Adduct modified clay

(AMC). The flow chart of polystyrene clay nanocomposite preparation using adduct modified clay was given in Figure 2.3.

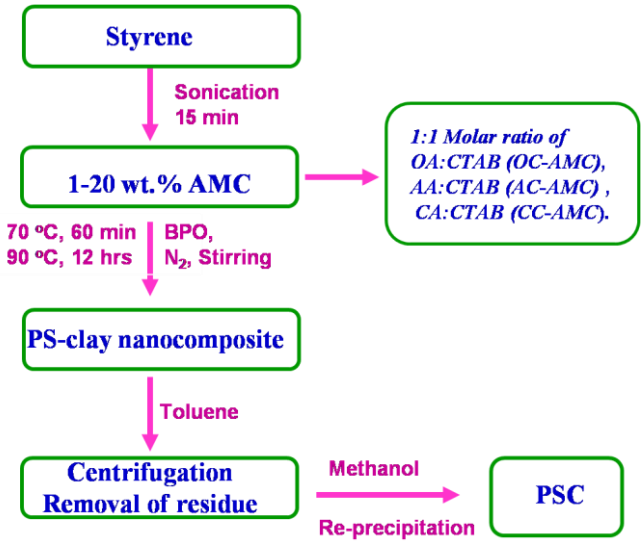

Figure 2.3. Flow chart for PSC preparation using adduct modified clay

For composite preparation, PSC loaded with 10 wt.% AMC were used since the maximum yield and better properties was obtained at this loading (Nair et al., 2010). The Styrene monomer (1.1ml) was charged into a round-bottom flask with 10 wt.% AC-AMC. The mixture was ultra sonicated for about 10 min to ensure proper dispersion of the clay. The flask was degassed with dry nitrogen for about 20 min prior to the addition of 2 wt.% BPO initiator. Polymerization was then carried out at 70°C by keeping in a temperature controlled oil bath under magnetic stirring (~500 rpm) for 3 h and then at 90°C for 10 h. The solid polystyrene attained was dispersed in a minimum amount of toluene, centrifuged to remove insoluble or suspended particles, and the soluble fraction was then precipitated in methanol. The precipitate was filtered and dried in vacuum

oven at temperature 60°C to obtain the polystyrene clay nanocomposite particle and was designated as PSC-AC10.

The same procedure was followed for the preparation of 10 wt.% PSC using CC-AMC and OC-AMC and the composites prepared were designated as PSC-CC10 and PSC-OC10, respectively.

2.3.3. Characterization Techniques

The functional group characterizations of modified organoclays were carried out using FT-IR spectroscopy, X-ray diffraction (XRD), and thermogravimetic analysis (TGA). And the nanocomposites were characterized using X-ray diffraction (XRD), thermogravimetic analysis (TGA) and Differential scanning calorimetry (DSC). FT-IR spectroscopy was carried out using a fully computerized Nicolet Impact 400D FT-IR spectrophotometer. Samples were mixed thoroughly with potassium bromide and compressed into pellets before recording. The extent of intercalation and exfoliation of AMC and PSC were characterized using WAXS and SAXS, respectively. WAXS and SAXS analysis were conducted on an XEUSS 2D SAXS/WAXS system using a Genix micro source from Xenocs operated at 50KV and 0.3 mA. The Cu-Kα radiation (λ=1.54Å) was collimated with an FOX2D mirror and two pairs of scatter less slits from Xenocs. The d-spacing of the materials were calculated from the angular position 2θ of the observed d_{hkl} reflection peaks based on the Bragg's formula $n\lambda = 2d\sin\theta$, where λ is the wavelength of the X-ray beam and θ is the diffraction angle. The measurements were performed over a 2θ range of 2° to 14°. Thermal stability measurements were performed at a

heating rate of 10°C/min from 40 to 800°C in a nitrogen atmosphere using Shimadzu, DTG-60 equipment. Differential scanning calorimetry was performed using Perkin Elmer Pyris 6 DSC calibrated using indium as standard and glass transition temperature was measured on second heating.

2.4. RESULTS AND DISCUSSION

As experimentally observed, the nanocomposite by the *in situ* intercalative polymerization, after removing the free polymer, contained soluble and insoluble fractions in toluene. The nanocomposite (PSC-AC) using the AC-AMC when compared to other modified clay, showed relatively higher yield of the soluble fraction, and exhibited better solvent-assisted self-assembling and anticorrosion properties and the details were discussed in chapter 3, 4 and 5.

Modification renders the clay layers more compatible with polymer chains and reduces the surface energy of clay layers and matches their surface polarity with the polymers (de Paiva et al., 2008). Well-dispersed nanocomposites are most likely to occur when a reactive functionality is incorporated in the organo-modified clay (Carastan and Demarquette, 2007; Nair et al., 2010).

2.4.1. FT-IR Spectroscopy

FT-IR spectroscopic studies support the successful intercalation of adduct onto the interlayer space of MMT. Figure 2.4 shows the FT-IR spectra obtained for both pristine clay and adduct modified clays.

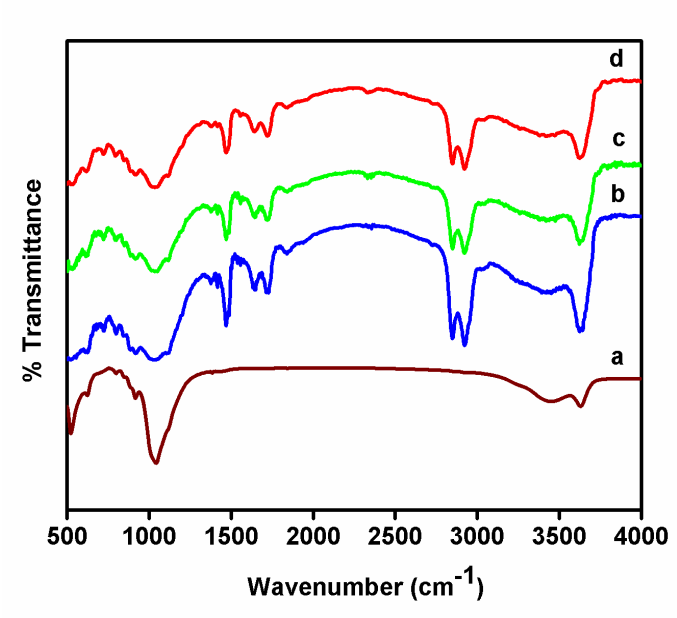

Figure 2.4. FT-IR spectra of (a) Pristine Na^+-MMT (b) AC-AMC (c) OC-AMC, and (d) CC-AMC

The unmodified clay showed bands due to Si–O–Si asymmetric stretching of silicate layer at 1028 cm^{-1} and structural hydroxyls at 3445cm^{-1}. For the modified clays, additional bands appeared due to the intercalation of organic moiety. In the case of AMC, the intense characteristic peaks at 2848 and 2926 cm^{-1} were observed due to the stretching vibration for $–CH_2$ and $–CH_3$, respectively. These absorption bands confirm the intercalation of the alkyl group of CTAB in the interlayer of all modified clay. The characteristic peak at 1642 cm^{-1} was assigned to C=C symmetric stretching of AC-AMC and OC-AMC, and C=C symmetric stretching of aromatic ring of CC-AMC was found at 1635 cm^{-1}. Moreover, characteristic peak at 1692 cm^{-1} was designated as C=O stretching for conjugated and aromatic acid group of AC-AMC and CC-AMC, respectively and characteristic peak found at 1716 cm^{-1} corresponded to the C=O stretching of saturated acid

group of OC-AMC. The changes in the characteristic peaks of the spectra for adduct modified clays indicate that the unmodified clay was almost entirely converted into the corresponding adduct modified clays.

2.4.2. XRD Analysis

Extent of the cationic exchange was further analyzed by WAXS, and the results were plotted in Figure 2.5.

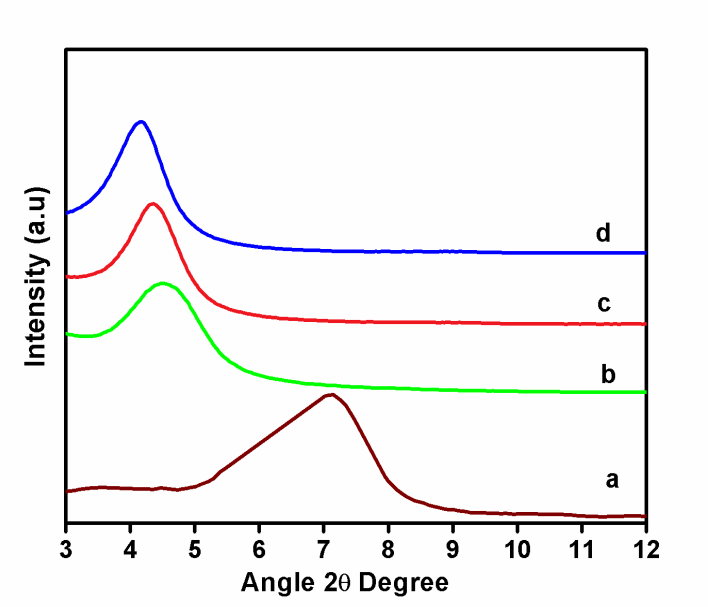

Figure 2.5. Wide-angle powder X-ray diffraction patterns of (a) pristine Na^+-MMT (b) OC-AMC, (c) CC-AMC and (d) AC-AMC

It was observed that the (001) reflection of all the AMC appeared at smaller angles (2θ) as compared to the pristine clay-indicating the successful ion exchange. The basal space increased from 1.24 nm (2θ = 7.12°) for pristine clay to a maximum of 2.12 nm (2θ = 4.16°) for AC-AMC. Similarly for CC-AMC and OC-AMC the basal spacing has increased to 2.03 nm (2θ = 4.35°) and 1.96 nm (2θ = 4.5°), respectively. These results clearly indicate that the increase in interlayer space was due to the inclusion of adduct

within the interlayer of the unmodified clay during the ion-exchange reaction.

It was visually observed that all the AMC swelled completely in styrene monomer and caused gelling of the solution upon the sonication. Gelation indicates the clay and styrene are chemically compatible for these organoclays, and swelling of clay in monomer indicates the compatibility of the clay with the monomer. It has been noted that higher the swelling the better dispersion of clay platelets in the final composite. Figure 2.6 shows the SAXS patterns of polystyrene clay nanocomposites with three different adducts at 10 wt.% clay loading.

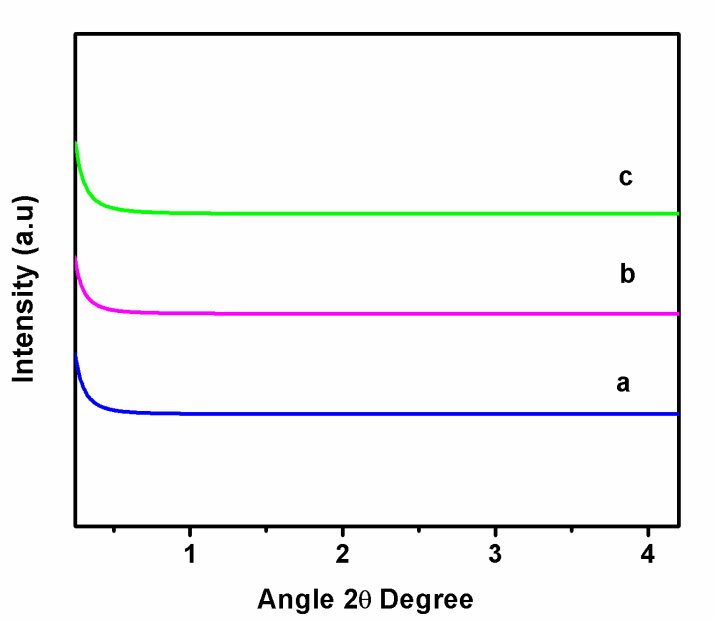

Figure 2.6. Small-angle powder X-ray diffraction patterns of (a) PSC-OC, (b) PSC-CC, and (c) PSC-AC

The disappearance of d_{001} peaks of all the PSCs indicates the formation of exfoliated nanocomposites. The absence of the 001 reflection suggests that the d_{001} value between the layered silicates is intercalated to spacing greater

than the measurable range, or clay layers are disorderly dispersed in the polystyrene matrix.

2.4.3. Thermogravimetric Analysis

TGA has been used usually to study the thermal decomposition behaviour of both modified clay and PSC. Figure 2.7A shows the thermogram of adduct modified clay.

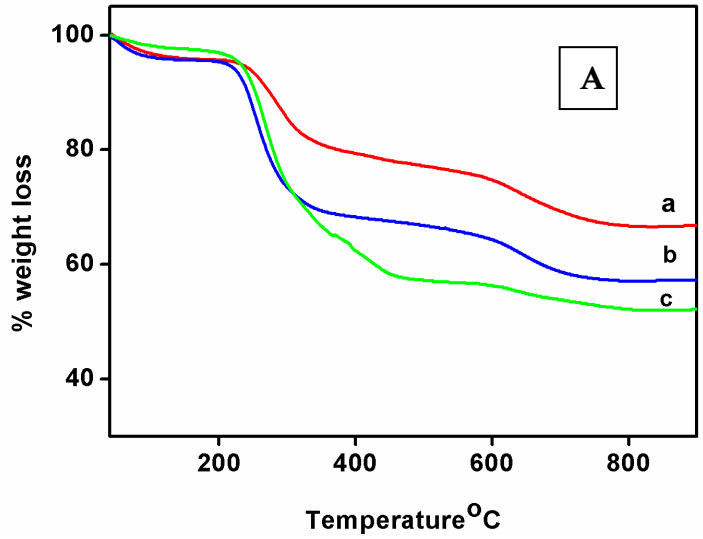

Figure 2.7A. TGA curve of modified clays (a) OC-AMC, (b) CC-AMC and(c) AC-AMC

From the TGA curve its clear that the organic constituents in the organoclay start to decompose at around 200°C. The highest temperature peak (500–800°C) is due to dehydroxylation of the clay layers. Comparing the residue at 800°C for the three adduct modified clay, the percentage polymeric residue was found to be 66% and remaining 34% was the inorganic content for AC-AMC. These indicates higher percentage incorporation of adduct into intergallery of Na^+ -MMT. This may also confirm the higher d-spacing observed in the case of AC-AMC. The

percentage polymeric residue at 800°C for CC-AMC and OC-AMC were found to be 57% and 52%, respectively.

Figure 2.7B shows typical thermogram of mass loss as a function of temperature for PS and the PSC materials. In general, there are several stages of weight loss starting from ~250°C and ending at 600°C, which might correspond to the degradation of the intercalating agent followed by the structural decomposition of the polymers. The relative thermal stability of the samples is compared in Table 2.1 and the onset degradation temperature (T_d - temperature at 10% mass loss) of PSC materials along with pristine PS is given. By the addition of AMC, evidently the onset thermal decomposition of all the PSC materials were shifted significantly towards the higher temperature range than that of pristine PS and was maximum for PSC-AC. After 600°C, all curves became flat and mainly the inorganic residue (i.e., Al_2O_3, MgO, SiO_2) remained.

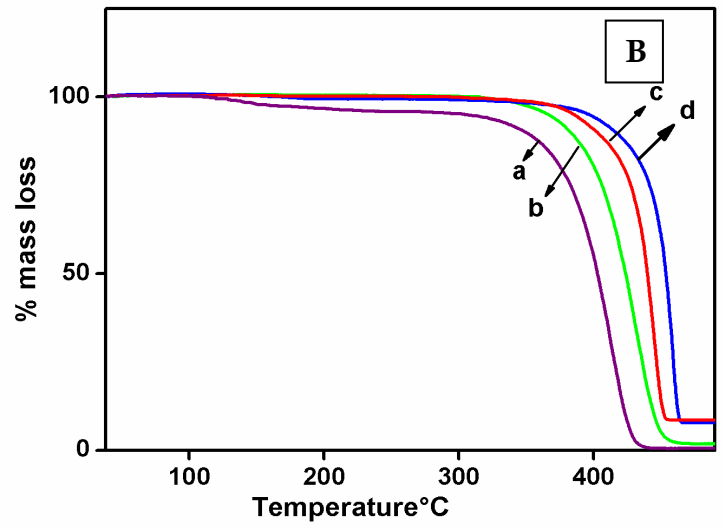

Figure 2.7B. TGA curves of (a) PS, (b) PSC-OC, (c) PSC-CC, and (d) PSC-AC

Table 2.1. Thermal property measurement of PS and PSC materials

Sample	Thermal Properties		
	Inorganic content [a] ***(wt.%)***	**T_d** [a] **(°C)**	**T_g** [b] **(°C)**
PS	-	347	76
PSC-AC	9.5	414	109
PSC-CC	9.1	382	104
PSC-OC	3.3	400	100

[a] *As determined by thermogravimetric analysis (TGA).*

[b] *As measured by differential scanning calorimetry (DSC)*

2.3.4. Differential scanning calorimetry

Thermal phase transition changes (e.g., glass transition temperature, T_g) of neat PS and PSC materials were studied by recording DSC at a heating rate of 10°C/min in a nitrogen atmosphere. Figure 2.8 shows the DSC scan of the entire sample, in which an endothermic shift in the baseline was observed. The T_g of all the PSC materials was significantly higher than that of pristine PS (Table 2.1). This result indicate that the portion of the intercalated PS chain segments within the interlayer spacing of clay tends to retard the segmental motion of the PS matrix and results in a T_g increase.

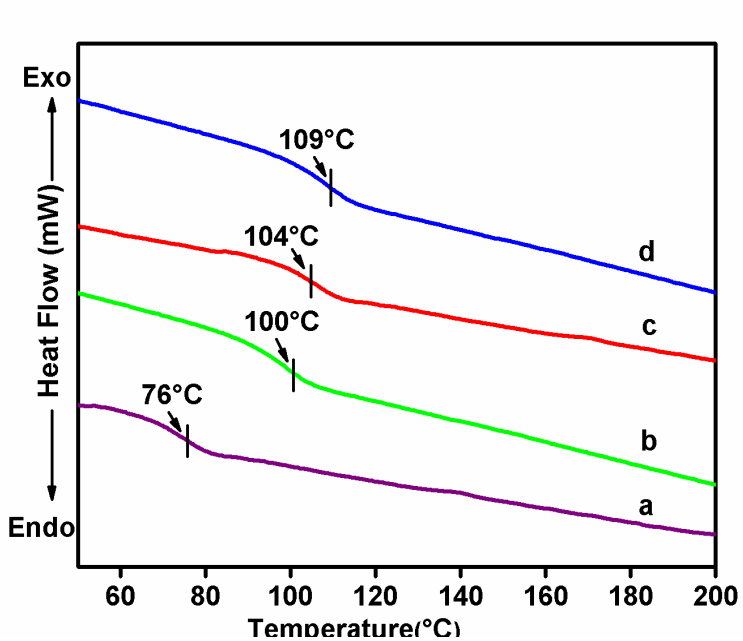

Figure 2.8. DSC curves of (a) PS, (b) PSC-OC, (c) PSC-CC, and (d) PSC-AC

2.3.5. Gel Permeation Chromatography

Molecular weights of the various polymer samples extracted from the nanolayers of MMT clays are obtained by Gel permeation chromatography (GPC) analysis. The molecular weights of the THF soluble polymer extracted from all the PSCs as well as bulk PS, were shown in Table 2.2. The molecular weights of extracted PS are found to be lower significantly than that of the bulk PS, implying the structurally restricted polymerization conditions existing in the intergallery region of the MMT clay. This can be attributed to difference in reactivity ratio of modified clay and styrene monomer when compared to reactivity between pristine styrene i.e. The rate of polymerisation reaction will be less as we increase the clay loading from 1 to 10 wt.%, which results in decrease in M_w and M_n and also results in increase in polydispersity.

Table 2.2. Molecular weights of bulk and extracted PS

Sample	M_w	M_n	Polydispersity
PS	68261	52916	1.29
PSC-AC1	62054	43394	1.43
PSC-AC3	51234	32426	1.58
PSC-AC5	44585	26697	1.67
PSC-AC10	35678	19390	1.84

[a] *As determined from GPC measurements.*

2.5. CONCLUSIONS

Adduct modified clay with different reactive acid group like acrylic acid, cinnamic acid and oleic acid, useful for the synthesis of PSC were prepared using Acid-CTAB adducts. FT-IR spectrum supports the successful intercalation of adducts into the interlayer space of MMT. This was further confirmed by XRD analysis, in which the (001) reflection of all the AMC appeared at smaller angles (2θ) as compared to the pristine clay-indicating the successful ion exchange. From XRD, AC-AMC showed a higher d-spacing (2.12 nm) compared to other AMC. This was confirmed by TGA of AMC, in which AC-AMC showed a higher polymeric residue of 66% compared to other adduct modified clays. Further the PSC-AC prepared using AC-AMC showed a higher thermal stability and higher glass transition temperature (T_g) compared to other adduct modified PSC. From GPC, it was found that the molecular weights of extracted PS are found to be lower significantly than that of the bulk PS, implying the structurally restricted polymerization conditions existing in the intergallery region of the MMT clay.